Inorganic Chemistry

Article

pubs.acs.org/IC

Design of One-Dimensional Coordination Networks from a Macrocyclic {3d-4f} Single-Molecule Magnet Precursor Linked by $[W(CN)_8]^{3-}$ Anions

Sébastien Dhers,[†] Humphrey L. C. Feltham,[†] Rodolphe Clérac,*[,‡,§] and Sally Brooker*[,†]

[†]Department of Chemistry and the MacDiarmid Institute for Advanced Materials and Nanotechnology, University of Otago, P.O. Box 56, Dunedin 9054, New Zealand

[‡]CNRS, CRPP, UPR 8641, F-33600 Pessac, France

[§]Univ. Bordeaux, CRPP, UPR 8641, F-33600 Pessac, France

Supporting Information

ABSTRACT: The outcome of 1:1 reactions of the tetranuclear 3d-4f Single Molecule Magnet (SMM) $[Cu_3Tb(L^{Pr})(NO_3)_2(H_2O)]NO_3$ (**1**) with $(TBA)_3[W(CN)_8]$ (TBA = tri-*n*-butyl ammonium cation, $[(n\text{-}Bu)_3N{-}H]^+$) in dimethylformamide (DMF) is dependent on the crystallization method employed: liquid−liquid diffusion of the reagents together gives $\{[Cu_3Tb(L^{Pr})W(CN)_8(DMF)_4]\cdot(DMF)\}_n$ (**2**) whereas diethyl ether vapor diffusion into the reaction solution gives $\{[Cu_3Tb(L^{Pr})W(CN)_8(DMF)_3(H_2O)_3]\cdot(DMF)_{1.5}\cdot(H_2O)_{0.5}\}_n$ (**3**). Both compounds are obtained as black single crystals and feature one-dimensional (1D) coordination networks (chains) of $[\mathbf{1}]^{3+}$ macrocycles linked by $[W(CN)_8]^{3-}$ anions. The two assemblies differ from a structural point of view. Complex **2** has a stepped arrangement with the linkers bound to the opposite faces of the macrocycle, whereas **3** has a square-wave arrangement due to the linkers binding to the same face of the macrocycle. Both compounds display an antiferromagnetic ground state below 3.5 and 2.4 K with a metamagnetic and antiferromagnetic (*T*, *H*) phase diagram for **2** and **3**, respectively. Remarkably the slow dynamics of the magnetization of the $[\mathbf{1}]^{3+}$ macrocycle units is preserved in **3** while this property is quenched in **2** because of stronger intra- and interchain magnetic interactions inducing a higher critical temperature.

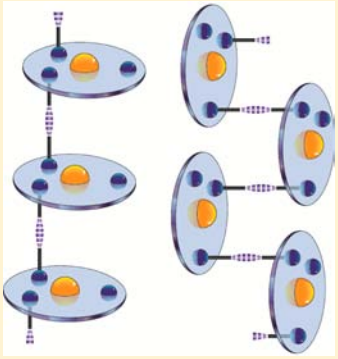

INTRODUCTION

Molecular magnetism using low-dimensional systems has been a rapidly expanding research area since the discovery in the early 1990s of the first Single-Molecule Magnet (SMM).[1] The discovery in 2001 of the first one-dimensional (1D) analogue,[2] subsequently named Single-Chain Magnet (SCM) behavior,[3] opened up further exciting possibilities, not least as the slow relaxation of the magnetization in SCMs is influenced not only by the magnetic anisotropy like in SMMs but also by intrachain magnetic interactions. Several SCMs have shown promising results and multifunctional SCMs have also been reported.[2,4] SMM and SCM compounds are therefore attractive objects for study in the fundamental sciences, for example, to explore quantum effects, and also for potential applications such as data storage.[5,6]

Macrocycles give the chemist significant control over the environment of the incorporated metal ions[7] but interestingly to date only a handful of SCMs have been synthesized from macrocyclic complexes.[8] In this paper, a tetranuclear 3d-4f macrocyclic complex, $[Cu_3Tb(L^{Pr})(NO_3)_2(H_2O)]NO_3$ (**1**) (Figure 1), that we have previously shown to be an SMM,[9] is employed as a building block to design coordination networks, aiming in particular to control the spatial organization of SMMs but also to form 1D networks that might show SCM properties. To link these macrocyclic complexes together we decided to use octacyanotungsten(V) anions (Figure 1), for several reasons. First because this coordinating unit is a trianion, so it will perfectly balance the charge in 1:1 complexes with the tricationic building block, $[Cu_3Tb(L^{Pr})]^{3+}$. In addition, cyanide bridges are known to be efficient coordinating linkers that also mediate significant exchange interactions between paramagnetic centers,[10] and cyanometallates have been used to successfully link heterometallic 3d-4f complexes of compartmental ligands into a 1D chain which exhibits SCM properties.[11] Moreover,

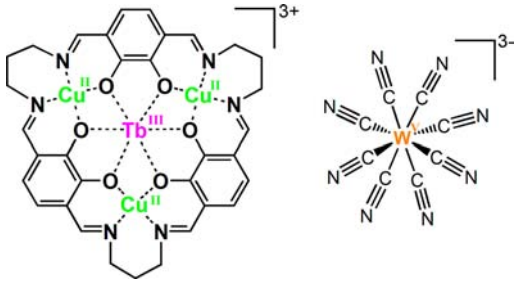

Figure 1. Schematic view of the building block moiety $[Cu_3Tb(L^{Pr})]^{3+}$ in **1** (left) and the linker $[W(CN)_8]^{3-}$ (right).

Received: September 4, 2013
Published: November 13, 2013

the type and strength of the magnetic interactions can be tuned by changing the 3d- or 4f-metal centers and ligands acting as spacers.[12]

Interest in octacyanometallates as linkers in molecular materials started more than a decade ago, with significant contributions from Sieklucka and co-workers,[12,13] as well as Sutter and co-workers,[8d,11,14] Okhoshi, Hashimoto, and co-workers,[4q,15] and Andruh and co-workers,[11,16] who between them have reported a wide range of compounds, from 0D to 3D networks.[12,13] Of the octacyanometallates, $[W^{V}(CN)_8]^{3-}$ has been shown to provide a greater exchange magnetic interaction than $[Mo^{V}(CN)_8]^{3-}$, because of 5d orbitals being more diffuse than 4d orbitals,[17] which is why we chose to focus on $[W^{V}(CN)_8]^{3-}$.

Prior to the present study, only a handful of 1D architectures that combine Cu^{II} and $[W^{V}(CN)_8]^{3-}$ had been reported, some of which are SCMs (Supporting Information, Table S1).[11,16a,18] Of these, two are particularly relevant to our present study. First $[Cu^{II}(cyclam)]_3[W^{V}(CN)_8]_2$, which is a ladder-like chain of macrocyclic copper(II) building blocks, where the octacyanotungstate linkers bind to *both* axial sites of an individual copper(II) center, but which does not show SCM properties.[18a] Second $[\{(Cu^{II}L)_2Ln\}\{W^{V}(CN)_8\}]$, which is a chain of $\{Cu^{II}_2Ln\}$ acyclic Schiff base complexes, related to our $\{Cu^{II}_3Tb\}$ macrocyclic complexes, with the linkers on opposing faces binding to *different* copper(II) centers and on one face also to the lanthanide(III) ion: this chain shows SCM properties (although the paper mainly describes the $\{Mo^{V}(CN)_8\}$ analogue).[11]

We report here that tuning the crystallization conditions employed for 1:1 reactions of our macrocyclic $\{Cu^{II}_3Tb\}$ building block **1** with a $[W(CN)_8]^{3-}$ linker in DMF permits the reproducible formation of two different 1D coordination assemblies which both feature identical 1:1 macrocycle to linker ratios, but which differ in structure and magnetic properties.

EXPERIMENTAL SECTION

Preparation of Compounds. Complex **1**[9] and $(TBA)_3[W(CN)_8]$[19] were prepared according to the literature methods.

*$\{[Cu_3Tb(L^{Pr})W(CN)_8(DMF)_4]\cdot(DMF)\}_n$ (**2**).* On top of a solution of **1** (5.5 mg, 4.3 μmol) in 10 mL DMF was layered a solution of $(TBA)_3[W(CN)_8]$ (4.1 mg, 4.2 μmol) in 10 mL DMF. Black single crystals of **2** grew over a few days and were filtered, washed with Et_2O and air-dried. Yield: 36% (2.6 mg, 1.5 μmol). IR $\bar{\nu}_{CN}$ (ATR, cm^{-1}) 2142 (m). Found (%): C, 37.42; H, 3.71; N, 14.68. Calculated for $C_{53}H_{64}Cu_3N_{18}O_{13}TbW$ ($[Cu_3Tb(L^{Pr})W(CN)_8(DMF)_4]\cdot(H_2O)_3$): C, 37.56; H, 3.81; N, 14.88.

*$\{[Cu_3Tb(L^{Pr})W(CN)_8(DMF)_3(H_2O)_3]\cdot(DMF)_{1.5}\cdot(H_2O)_{0.5}\}_n$ (**3**).* Complex **1** (36.8 mg, 28.8 μmol) and $(TBA)_3[W(CN)_8]$ (27.7 mg, 28.6 μmol) were taken up in 100 mL of DMF. The solution was stirred for 30 minutes before Et_2O was vapor diffused into the solution. Black single crystals of **3** grew over a few days and were filtered, washed with DMF and Et_2O, and air-dried. Yield: 32.5% (15.6 mg, 9.3 μmol). IR $\bar{\nu}_{CN}$ (ATR, cm^{-1}) 2133 (m). Found (%): C, 35.75; H, 3.86; N, 14.03. Calculated for $C_{50}H_{63}Cu_3N_{17}O_{15}TbW$ ($[Cu_3Tb(L^{Pr})W(CN)_8(DMF)_3(H_2O)_3]\cdot(H_2O)_3$): C, 35.84; H, 3.79; N, 14.21.

X-ray Structure Determinations. Both compounds were obtained as single crystals so X-ray data collections were carried out, on a Bruker SMART Apex II diffractometer using graphite-monochromated Mo-*K*a radiation (λ = 0.71073 Å). Structure solution and full-matrix least-squares refinement were carried out using the SHELXTL software package.[20] For **2**, no disorder was present. All non-hydrogen atoms were refined anisotropically except for one carbon atom in one of the coordinated DMF molecules and all of the atoms of the two noncoordinated DMF molecules. For **3**, all non-hydrogen atoms were refined anisotropically except for all of the solvent molecules. One of the 1.5 noncoordinated DMF molecules was modeled over two sites (0.75:0.25 occupancy), while the other was 0.5 occupancy. Table 1 summarizes the unit cell and structure refinement parameters for compounds **2** and **3**. Supporting Information, Figures S1–S3 give different views of the crystal packing and the weak interchain contacts. The cif files are available from the Cambridge Structural Database: CCDC 958791 (**2**) and 958792 (**3**).

Table 1. Unit Cell and Structure Refinement Parameters for Compounds 2 and 3

	2	3
formula	$C_{56}H_{63}Cu_3N_{19}O_{11}TbW$	$C_{54.5}H_{68.5}Cu_3N_{18.5}O_{14}TbW$
molecular weight ($g\ mol^{-1}$)	1711.64	1740.17
T (K)	92	93
crystal system	triclinic	monoclinic
space group	$P\bar{1}$	$P2_1/c$
Z	2	4
a (Å)	14.4966(8)	22.615(7)
b (Å)	15.1538(8)	14.423(4)
c (Å)	17.8509(9)	19.720(6)
α (deg)	73.872(3)	90
β (deg)	81.949(3)	92.276(14)
γ (deg)	62.803(2)	90
V (Å^3)	3350.2(3)	6427(3)
$\rho_{calcd.}$ ($g\ cm^{-3}$)	1.697	1.798
R_1	0.0513	0.0494
wR_2	0.1484	0.1264

Magnetic Properties. The magnetic susceptibility measurements were carried out using an MPMS-XL Quantum Design SQUID magnetometer operating between 1.8 and 400 K for direct current (dc) applied fields ranging from −70 to 70 kOe at about 100 to 400 Oe/min. Alternating current (ac) susceptibility experiments were realized at ac frequencies ranging from 1 to 1500 Hz with an ac field amplitude of 3 Oe. Measurements were performed on air-dried analytically pure polycrystalline samples (21.15 and 6.470 mg for **2** and **3**) which were loaded into a sealed polyethylene bag (3 × 0.5 × 0.02 cm). The magnetic data were corrected for the sample holder and the diamagnetic contributions.

RESULTS AND DISCUSSION

Depending on the crystallization method employed, the 1:1 reactions of $[Cu_3Tb(L^{Pr})(NO_3)_2(H_2O)]NO_3$ (**1**) with $(TBA)_3[W(CN)_8]$ in DMF give black single crystals of two different compounds, $\{[Cu_3Tb(L^{Pr})W(CN)_8(DMF)_4]\cdot(DMF)\}_n$ (**2**) and $\{[Cu_3Tb(L^{Pr})W(CN)_8(DMF)_3(H_2O)_3]\cdot(DMF)_{1.5}\cdot(H_2O)_{0.5}\}_n$ (**3**). Crystals of **2** are obtained by slow liquid–liquid diffusion of the two reagent solutions together, whereas crystals of **3** are obtained by vapor diffusion of diethyl ether into a solution of the reagents. Both compounds have the same molecular ratio, one macrocyclic building block per molecule of tungsten(V) octacyanide linker, and have been structurally characterized by X-ray crystallography (Figures 2–4). In both structures, **2** and **3**, the macrocycle adopts a slightly curved conformation, coordinating one Tb^{III} in the O_6 pocket and three Cu^{II} in the N_2O_2 sites (Figures 1 and 2, Table 2). In **2**, all three Cu^{II} ions possess a square-pyramidal geometry whereas in **3** only one Cu^{II} ion is square-pyramidal while the other two are octahedral. The Tb^{III} ion is coordinated by nine oxygen atoms, six from the macrocycle and three from water or DMF molecules. The geometry of the Tb^{III} ion has been

dx.doi.org/10.1021/ic402248y | Inorg. Chem. 2013, 52, 13685–13691

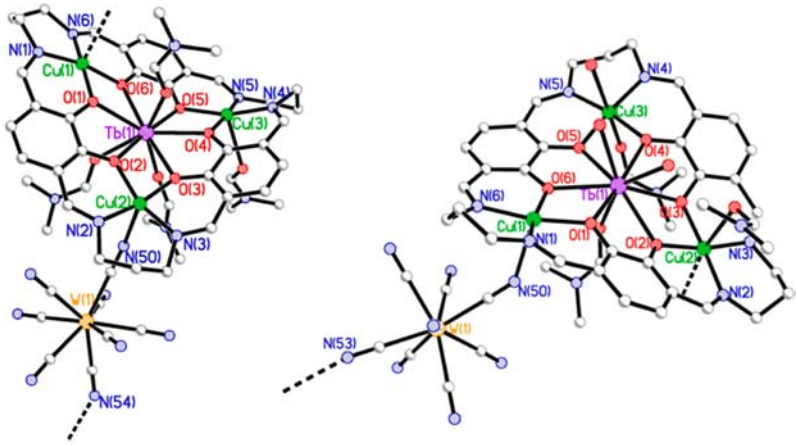

Figure 2. Asymmetric unit for complex **2** (left) and complex **3** (right) and their atom numbering schemes. All hydrogen atoms and non-coordinating solvent molecules omitted for clarity.

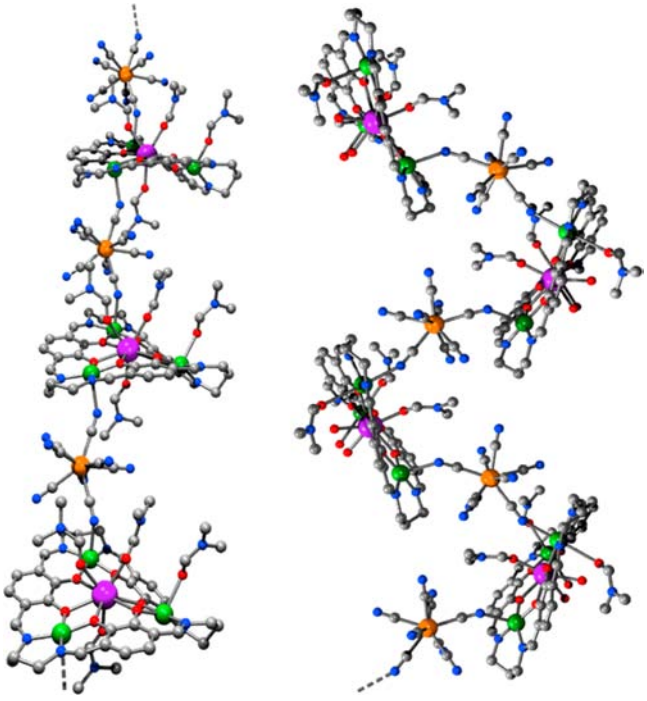

Figure 3. Views of the 1D coordination network in **2** (left) and **3** (right) emphasizing the stepped chain (left) and the square wave chain (right) assemblies, respectively. All hydrogen atoms and non-coordinating solvent molecules omitted for clarity. Tb (purple), Cu (green), W (orange), N (blue), O (red), and C (gray) atoms are represented in the colors indicated in brackets.

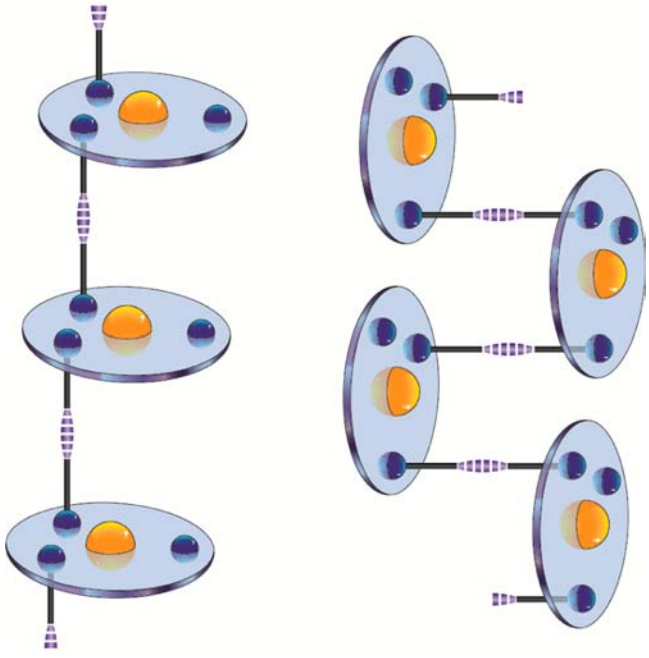

Figure 4. Schematic view of the 1D coordination network in **2** (left) and **3** (right) emphasizing the stepped chain (left) and the square wave chain (right) assemblies, respectively.

analyzed with the SHAPE program (Supporting Information, Table S2),[21] revealing a hula-hoop geometry in both **2** and **3** (Supporting Information, Figure S4). This is a common geometry for hexadentate macrocyclic ligands where the six donors are forced to remain coplanar,[22] which is the case for our macrocycle. The geometry of the W^V in the $[W(CN)_8]^{3-}$ fragment has also been analyzed with the SHAPE program (Supporting Information, Table S3),[21] revealing a square antiprismatic geometry in **2** and a dodecahedral geometry in **3** (Supporting Information, Figure S5). Both geometries are commonly encountered for the $[W(CN)_8]^{3-}$ fragment.[13a] In both **2** and **3**, two *different* Cu^{II} centers per tetrametallic macrocycle, Cu(1) and Cu(2), bind to the two $[W(CN)_8]^{3-}$ linkers, forming the chains; however, they differ in that in **2** the two linkers bind to *opposite faces* of the macrocycle whereas in **3** they both bind on the *same face* of the macrocycle (Figures 2−4). As is discussed below, this results in two distinctly different 1D chain structures and consequently **2** and **3** also differ in magnetic behavior.

The structure determination of **2** revealed that the 1D coordination assembly is composed of alternating linker anions and macrocycle cations with the macrocycles arranged in a "stepped" fashion (Figure 3a), each with two linkers bound to *opposite faces* of the macrocycle. Two of the three copper(II) ions are bound to the tungsten(V) octacyanide linker (Figure 2) through axial coordination of the nitrogen atoms of the cyanide ligands (Cu1−N54 = 2.424 Å and Cu2−N50 = 2.425 Å), one being a perfectly regular square pyramid (trigonality factor[23] $\tau_{Cu2} < 0.01$) while the other is slightly distorted toward trigonal bipyramidal (trigonality factor $\tau_{Cu1} = 0.14$). This is

dx.doi.org/10.1021/ic402248y | *Inorg. Chem.* 2013, 52, 13685−13691

Table 2. Comparison of Geometries of M Centers, Selected Bond Lengths (Å), Bond Angles (deg), and M−M′ Distances (Å) for Compounds 1−3, Provided as Range (*Average*). The M−M′ Separations Quoted Are the Shortest

	1[9]	2	3
Cu geometries	square pyramidal	square pyramidal	square pyramidal/octahedral[b]
τ(Cu)	0.001−0.170 (*0.063*)	0.004−0.25 (*0.131*)	0.139[b]
Cu−N_{imine}	1.951−1.985 (*1.972*)	1.948−2.009 (*1.977*)	1.964−2.000 (*1.985*)
Cu−O_{cat}	1.915−1.944 (*1.927*)	1.895−1.966 (*1.941*)	1.925−1.963 (*1.949*)
Cu−X_{axial}[a]	2.324−2.534 (*2.429*)	2.405	2.504−2.785 (*2.631*)
Cu−$N_{cyanide}$		2.424−2.425 (*2.425*)	2.508−2.512 (*2.510*)
Tb geometry	hula-hoop	hula-hoop	hula-hoop
Tb−O_{cat}	2.407−2.464 (*2.439*)	2.449−2.505 (*2.476*)	2.405−2.533 (*2.479*)
Tb−O_{axial}	2.484−2.513 (*2.499*)	2.335−2.431 (*2.392*)	2.291−2.482 (*2.387*)
Cu···Cu (intra)	6.108	6.189	6.315
Cu···Tb (intra)	3.585	3.639	3.629
Cu···Cu (intrachain)		10.928	10.489
Cu···Cu (intermolecular)	7.581	6.596	6.403
Tb···Tb (intrachain)		15.154	14.894
Tb···Tb (intermolecular)	8.593	9.420	10.385
W geometry		square antiprismatic	dodecahedral
W···Cu (intra)		5.484	5.479
W···Cu···W angle		165.99	139.09
Cu···C···N angle		145.82−147.87 (*146.85*)	141.32−155.81 (*148.57*)
W···C···N angle		176.67−177.73 (*177.2*)	176.38−179.05 (*177.72*)
Ph−Ph angle within L^{Pr}	21.86−34.97 (*27.54*)	16.53−37.96 (*30.49*)	25.68−33.29 (*29.62*)

[a]X_{axial} for Cu = MeOH and NO_3^- for **1**, DMF for **2**, DMF and H_2O for **3**. [b]Only Cu1 is square pyramidal in **3**.

unfortunate with regard to the possibility of effective magnetic exchange along the chains because (a) the linkers do not bind to *both axial* sites of an individual copper(II) center and (b) the approximate square pyramidal geometries imply that the magnetic orbital of the copper(II) centers will lie in the plane of the macrocycle so magnetic exchange interactions via the axially bound linker can be expected to be weak (see later). The third copper(II) ion is bonded to a DMF molecule (Cu3−O_{DMF} = 2.405 Å) giving a distorted square-pyramidal geometry (trigonality factor[23] τ_{Cu3} = 0.25). The stepped chains pack together efficiently via nonclassical C−H-bond interactions,[24] resulting in a 3D network (N55−C71 = 3.296 Å, C28−O80 = 3.560 Å, C22−N52 = 3.239 Å, Supporting Information, Figure S1). The Tb−Tb separation is far shorter interchain (9.420 Å) than intrachain (15.154 Å). Likewise the Cu−Cu separation is far shorter interchain (6.596 Å) than intrachain (10.928 Å), but is longer than that observed within the macrocycle (6.189 Å, Table 2).

In contrast, in **3** the macrocycles are packed in a "square-wave" fashion, each with two linkers bound to the *same face* of the macrocycle (Figure 3b). Two of the three copper(II) ions are bound to the tungsten(V) octacyanide complex through axial coordination of the nitrogen atoms of the cyanide ligands (Cu1−N50 = 2.508 Å and Cu2−N53 = 2.512 Å), one with a square pyramidal geometry slightly distorted toward trigonal bipyramidal (trigonality factor τ_{Cu1} = 0.139) and the other with an octahedral environment with a Jahn−Teller distortion (Figure 2, Table 2). As in **2**, the linkers do not bind to both axial sites of the same copper(II) center, and the square plane of strong macrocycle donors to the two different copper(II) centers involved place the magnetic orbitals in the plane of the macrocycle, so again magnetic coupling along the chain can be expected to be weak (see later). The third copper(II) ion is bonded to a DMF molecule (Cu3−O_{DMF} = 2.504 Å) and a water molecule (Cu3−O_{H2O} = 2.604 Å) giving an octahedral geometry with a Jahn−Teller distortion (Table 2). Again the chains pack together efficiently side-by-side, but this time via classical H-bond interactions between a cyanide moiety and a coordinated water molecule on an adjacent chain, resulting in a 2D sheet of H-bonded chains (O11−N54′ = 2.974 Å, Supporting Information, Figure S2). These sheets interact by nonclassical H-bonds between another cyanide moiety and a coordinated DMF on another chain (C81′−N56 = 3.131 Å, Supporting Information, Figure S3), alternately above and below, giving a 3D network overall. The Tb−Tb separation is far shorter interchain (10.385 Å) than intrachain (14.894 Å). Likewise the Cu−Cu separation is far shorter interchain (6.403 Å) than intrachain (10.489 Å), but is longer than that observed within the macrocycle (6.315 Å, Table 2).

The static magnetic properties of **2** and **3** have been studied and are shown in Figure 5 (black and red data points, respectively; almost completely overlapping until very low temperatures) as the temperature dependence of the χT product at 1000 Oe. The χT value at room temperature is equal to 13.6 cm^3 K mol^{-1} for both **2** and **3**, respectively, which is in good agreement with the expected χT value of 13.315 cm^3 K mol^{-1} calculated for three Cu^{II} (S = 1/2; g = 2.0; C = 0.375 cm^3 K mol^{-1}), one W^V (S = 1/2; g = 2.0; C = 0.375 cm^3 K mol^{-1}), and one Tb^{III} (S = 3, L = 3, $^7F_6$, g = 3/2, C = 11.815 cm^3 K mol^{-1}). It is also worth mentioning that the room temperature χT product for the 1D compounds is in accord with the value estimated from the magnetic data of the components: the discrete macrocyclic SMM **1** (blue data in Figure 5, χT (270 K) = 13 cm^3 K mol^{-1}) plus a paramagnetic contribution from the S

dx.doi.org/10.1021/ic402248y | Inorg. Chem. 2013, 52, 13685−13691

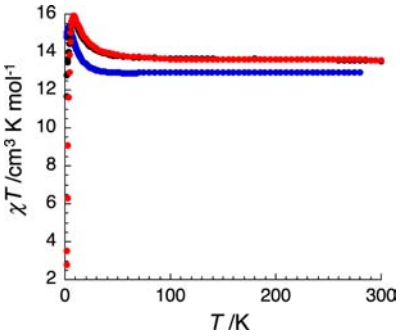

Figure 5. Temperature dependence of the χT product for **1** (blue dots), **2** (black dots), and **3** (red dots) at 1000 Oe (χ is the molar magnetic susceptibility defined as M/H per mole of repeat unit).

= 1/2 W^V magnetic center in the linker. When the temperature is decreased, the χT product is roughly constant down to 50 K before exhibiting a slow increase up to 15.5 and 15.9 cm^3 K mol^{-1} at 7.7 and 8.2 K for **2** and **3**, respectively. This thermal behavior is typical of *dominant ferromagnetic interactions* between the Cu^{II} and Tb^{III} spin carriers, as already observed in **1** (Figure 5).[9] Further decreases down to 11.6 and 2.8 cm^3 K mol^{-1} at 1.8 K for **2** and **3**, respectively, indicate the combined presence of magnetic anisotropy and *intermolecular antiferromagnetic interactions*, which lead to antiferromagnetic orders (vide infra). Nevertheless, it is important to note that the magnetic properties of **2** and **3** are extremely similar to **1** (roughly a simple shift by the paramagnetism of the S = 1/2 W^V magnetic center in Figure 5) indicating that the *couplings along and between the 1D coordination networks are weak and smaller (in absolute value) than the Cu−Tb magnetic interaction.*

For both compounds, the field dependence of the magnetization exhibits a typical "*S*" shaped curve (i.e., with an inflection point at H_C; Supporting Information, Figures S6−S7 and S9−S10) at 1.8 K that reveals the presence of antiferromagnetic interactions compensated by the applied magnetic field at H_C. This characteristic field has been followed as a function of the temperature using combined M vs H and χ vs T data (Supporting Information, Figures S6−S11) and taking the maximum of the dM/dH vs H and χ vs T plots. Using this approach, the (T, H) magnetic phase diagrams have been built (Figure 6). The extrapolation of the characteristic field to zero at a finite temperature proves in both compounds the presence of an 3D antiferromagnetic order with T_N = 3.5 and 2.4 K for **2** and **3**, respectively. The topology of the obtained phase diagram for **2** is typical of a metamagnetic behavior with only an antiferromagnetic−paramagnetic phase transition. In the case of **3**, a second inflection point, that is, characteristic field, is observed at higher field (Supporting Information, Figure S10, around 2100 Oe at 1.83 K) suggesting the presence of a spin-flop phase between the low field 3D antiferromagnetic ordered state and the paramagnetic phase (antiferromagnetic phase diagram). The origin of the different phase diagrams is found in the magnetic anisotropy of the systems: weak anisotropy leads to an antiferromagnetic phase diagram for **3** and strong magnetic anisotropy leads to a metamagnetic phase diagram for **2**.[25] It is relatively straightforward to think that the different packing of the $[Cu_3Tb(L^{Pr})]^{3+}$ anisotropic complexes (Figures 3 and 4) might be responsible for the reduction of the magnetic anisotropy in **3** in comparison with **2**, but it is not possible to rule out that the change in the Tb^{III} coordination sphere between **2** and **3** might

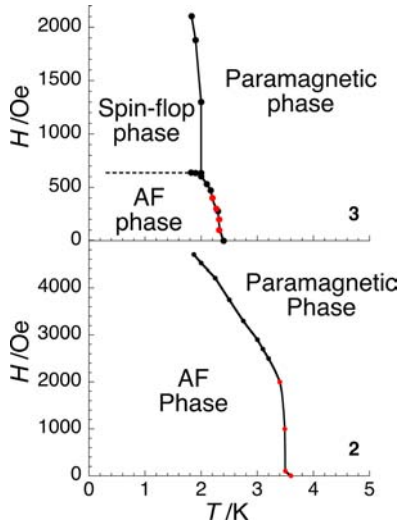

Figure 6. Magnetic phase diagram (T,H) of **2** (bottom) and **3** (top) constructed from χ vs T (red dots) and M vs H (black dots) data (Supporting Information, Figures S6−S11). The solid black line is a guide for the eye.

also play a key role. Moreover the higher T_N and H_C (at 1.8 K) in **2** indicates slightly stronger intra- and interchain interactions in **2** than in **3**. Unfortunately because of the complexity of the systems in terms of magnetic centers (number and nature), magnetic interactions and anisotropy, it is obviously impossible to estimate these microscopic magnetic parameters from the experimental data and thus the analysis of the magnetic properties has to stay qualitative.

While for **2** the ac susceptibility measurements revealed a total absence of out-of-phase ac signal (χ'') in zero or in dc applied magnetic field, compound **3** exhibits a clear nonzero χ'' component below 4 K even in zero-dc field (Supporting Information, Figures S12−S13), comparable with that observed for the SMM unit **1**.[9] This slow relaxation of the magnetization was studied as a function of the temperature below 4 K and the ac frequency between 1 and 1500 Hz. Unfortunately in zero-dc field, no clear maximum of the χ'' vs T or χ'' vs ν data is observed, so it is not possible to experimentally determine the temperature dependence of the characteristic time of the magnetization relaxation at zero-dc field. Therefore as often done for SMMs, to lift the states degeneracy and thus minimize the probability of the fast quantum tunneling of the magnetization, the slow dynamics observed for **3** has been studied in presence of a small dc field (Supporting Information, Figures S14 and S15). It is worth noting that in the ordered magnetic phase below 2.4 K (Figure 6), the applied dc-field also helps to compensate the intercomplex magnetic interactions and thus to decouple the SMM building-blocks to reveal their intrinsic dynamics.[26] As expected for a SMM in a relaxation regime influenced by quantum tunneling and intermolecular interactions, the relaxation mode is slightly shifted to lower frequencies allowing the clear detection of a maximum in the χ'' vs ν data (Supporting Information, Figure S14). The relaxation time of **3** has thus been studied at 800 Oe as that appears to be a dc field at which there is a good compromise between the intensity of the relaxation mode and the frequency shift is obtained (Supporting Information, Figure S15). At 800 Oe, χ'' vs T or χ'' vs ν data have been collected (Supporting Information, Figures S16 and S17) and the relaxation time has been deduced between 1.88 and 2.6 K from the maxima of

dx.doi.org/10.1021/ic402248y | Inorg. Chem. 2013, 52, 13685−13691

the $\chi''(\nu)$ curves at a given temperature, for which $\tau = 1/(2\pi\nu_{max})$, and, for the data where a maximum could not be observed, by applying a classical scaling method (Supporting Information, Figure S18).[27] As shown in the inset of Figure 7,

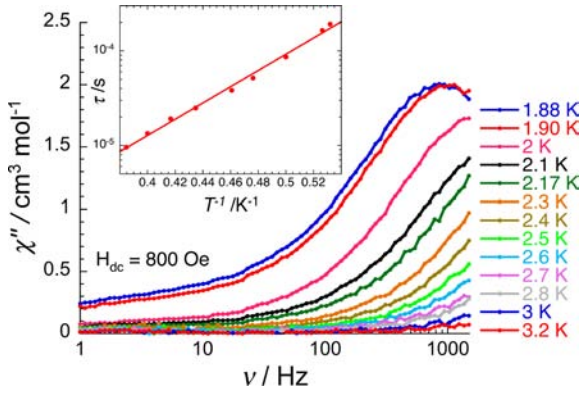

Figure 7. Frequency dependence of the imaginary (χ'') part of the ac susceptibility for **3** in 800-Oe dc field at different temperatures between 1.82 and 3.2 K. Inset: τ vs T^{-1} plot for **3** in 800-Oe dc field. The solid line is the best fit to the Arrhenius law discussed in the text.

the relaxation time is thermally activated in this temperature region with an energy gap of 20(1) K ($\tau_0 = 4.7 \times 10^{-9}$ s), similar to the butylene analogue of **1**, $[Cu_3TbL^{Bu}]^{3+}$ (Δ_{eff}/k_B = 19.5 K, $\tau_0 = 3.4 \times 10^{-7}$ s).[28] The presence of the slow relaxation of magnetization in the antiferromagnetic ordered phase of **3** is not surprising as it has been also observed for ordered systems incorporating two-dimensional networks of SMM building-blocks or Single-Chain Magnets.[4f,26a,29] In **3**, the coupling between the SMM building blocks, $[Cu_3Tb(L^{Pr})]^{3+}$, is sufficiently strong to stabilize a magnetic order at 2.4 K, but the intrinsic slow dynamics of the SMM units is possible above and below the critical temperature (2.4 K). In contrast, it seems that the stronger couplings, both along and between the chains, inducing the antiferromagnetic order in **2** (Figure 6), do not allow the persistence of the intrinsic slow dynamics of the $[Cu_3Tb(L^{Pr})]^{3+}$ moieties in **2**.

In conclusion, we have successfully prepared two different 1D coordination networks of the $[Cu_3Tb(L^{Pr})]^{3+}$ SMM by employing a rational and controlled building block approach. The selection of the trianionic $[W(CN)_8]^{3-}$ linker provided charge balance and thus facilitated the formation of these 1:1 chains. Depending on the crystallization methods employed, black crystals of stepped (**2**) or square-wave (**3**) chains were reproducibly obtained. The different structural motifs result in differing magnetic behavior: **2** and **3** display respectively a metamagnetic and antiferromagnetic phase diagram. While in **2** the antiferromagnetic order at 3.5 K blocks the slow dynamics of the individual $[Cu_3Tb(L^{Pr})]^{3+}$ units, the weaker intra- and interchain interactions in **3** allow the slow relaxation of the magnetization, similar to **1** (with an energy gap around 20 K), even in the ordered states. These results show that the magnetic information is not being communicated efficiently enough between the $[Cu_3Tb(L^{Pr})]^{3+}$ units, along these 1D coordination networks, to obtain Single-Chain Magnet properties. To generate systems with enhanced linker-macrocycle magnetic interactions two factors should be addressed: (a) choice of a better $[M_3Ln(L)]^{3+}$ building block, one in which the magnetic orbitals of M are at right angles to the macrocycle thereby facilitating overlap with the linker and hence magnetic exchange, and (b) choice of a more appropriate linker. We are investigating both of these avenues, as well as looking to instead link the Ln ions, as we attempt to generate new SCMs from macrocyclic SMM building blocks by maximizing the intrachain interactions and, at the same time, minimizing the interchain contacts.

■ ASSOCIATED CONTENT

Supporting Information

Summary of key data on related literature complexes; additional X-ray crystal structure diagrams and magnetochemistry plots for complexes **2** and **3**. This material is available free of charge via the Internet at http://pubs.acs.org.

■ AUTHOR INFORMATION

Corresponding Authors

*E-mail: clerac@crpp-bordeaux.cnrs.fr. Fax: (+33) 5 56 84 56 00. Phone: (+33) 5 56 84 56 50.

*E-mail: sbrooker@chemistry.otago.ac.nz. Fax: (+64) 3 479 7906. Phone: (+64) 3 479 7919.

Notes

The authors declare no competing financial interest.

■ ACKNOWLEDGMENTS

This work was supported by grants from the University of Otago and the MacDiarmid Institute for Advanced Materials and Nanotechnology (including a Ph.D. scholarship for S.D.). We also thank the University of Bordeaux, the CNRS, the Région Aquitaine, the ANR and the Dumont d'Urville NZ-France Science & Technology Support Programme (No. 23793PH).

■ REFERENCES

(1) (a) Sessoli, R.; Gatteschi, D.; Caneschi, A.; Novak, M. A. *Nature* **1993**, *365*, 141. (b) Sessoli, R.; Tsai, H.-L.; Schake, A. R.; Wang, S.; Vincent, J. B.; Folting, K.; Gatteschi, D.; Christou, G.; Hendrickson, D. N. *J. Am. Chem. Soc.* **1993**, *115*, 1804.

(2) Caneschi, A.; Gatteschi, D.; Lalioti, N.; Sangregorio, C.; Sessoli, R.; Venturi, G.; Vindigni, A.; Rettori, A.; Pini, M. G.; Novak, M. A. *Angew. Chem., Int. Ed.* **2001**, *40*, 1760.

(3) Clérac, R.; Miyasaka, H.; Yamashita, M.; Coulon, C. *J. Am. Chem. Soc.* **2002**, *124*, 12837.

(4) See for example: (a) Lescouezec, R.; Vaissermann, J.; Ruiz-Perez, C.; Lloret, F.; Carrasco, R.; Julve, M.; Verdaguer, M.; Dromzee, Y.; Gatteschi, D.; W., W. *Angew. Chem., Int. Ed.* **2003**, 1521. (b) Wang, S.; Zuo, J.-L.; Gao, S.; Song, Y.; Zhou, H.-C.; Zhang, Y.-Z.; You, X.-Z. *J. Am. Chem. Soc.* **2004**, *126*, 8900. (c) Xu, H.-B.; Wang, B.-W.; Pan, F.; Wang, Z.-M.; Gao, S. *Angew. Chem., Int. Ed.* **2007**, *46*, 7388. (d) Miyasaka, H.; Saitoh, A.; Yamashita, M.; Clérac, R. *Dalton Trans.* **2008**, 2422. (e) Ouellette, W.; Prosvirin, A. V.; Whitenack, K.; Dunbar, K. R.; Zubieta, J. *Angew. Chem., Int. Ed.* **2009**, *48*, 2140. (f) Miyasaka, H.; Takayama, K.; Saitoh, A.; Furukawa, S.; Yamashita, M.; Clérac, R. *Chem.—Eur. J.* **2010**, *16*, 3656. (g) Hoshino, N.; Sekine, Y.; Nihei, M.; Oshio, H. *Chem. Commun.* **2010**, *46*, 6117. (h) Liu, T.; Zhang, Y.-J.; Kanegawa, S.; Sato, O. *J. Am. Chem. Soc.* **2010**, *132*, 8250. (i) Harris, T. D.; Bennett, M. V.; Clérac, R.; Long, J. R. *J. Am. Chem. Soc.* **2010**, *132*, 3981. (j) Feng, X.; David Harris, T.; Long, J. R. *Chem. Sci.* **2011**, *2*, 1688. (k) Yoon, J. H.; Ryu, D. W.; Choi, S. Y.; Kim, H. C.; Koh, E. K.; Tao, J.; Hong, C. S. *Chem. Commun.* **2011**, *47*, 10416. (l) Nather, C.; Boeckmann, J. *Chem. Commun.* **2011**, *47*, 7104. (m) Dong, D.-P.; Liu, T.; Kanegawa, S.; Kang, S.; Sato, O.; He, C.; Duan, C.-Y. *Angew. Chem., Int. Ed.* **2012**, *51*, 5119. (n) Senapati, T.; Pichon, C.; Ababei, R.; Mathonière, C.; Clérac, R. *Inorg. Chem.* **2012**, *51*, 3796. (o) Miyasaka, H.; Madanbashi, T.; Saitoh, A.; Motokawa, N.; Ishikawa, R.; Yamashita, M.; Bahr, S.; Wernsdorfer, W.; Clérac, R.

Chem.—Eur. J. **2012**, *18*, 3942. (p) Zhang, W.-X.; Shiga, T.; Miyasaka, H.; Yamashita, M. *J. Am. Chem. Soc.* **2012**, *134*, 6908. (q) Chorazy, S.; Nakabayashi, K.; Imoto, K.; Mlynarski, J.; Sieklucka, B.; Ohkoshi, S.-i. *J. Am. Chem. Soc.* **2012**, *134*, 16151.
(5) Gatteschi, D.; Sessoli, R.; Villain, F. *Molecular Nanomagnets*; Oxford University Press: Oxford, U.K., 2006.
(6) (a) Leuenberger, M. N.; Loss, D. *Nature* **2001**, *410*, 789. (b) Jeon, I.-R.; Clérac, R. *Dalton Trans.* **2012**, *41*, 9569.
(7) Useful reviews include: (a) Lindoy, L. F.; Park, K.-M.; Lee, S. S. *Chem. Soc. Rev.* **2013**, *42*, 1713. (b) Vigato, P. A.; Peruzzo, V.; Tamburini, S. *Coord. Chem. Rev.* **2012**, *256*, 953. (c) Love, J. B. *Chem. Commun.* **2009**, 3154. (d) Brooker, S. *Coord. Chem. Rev.* **2001**, *222*, 33. (e) Gerbeleu, N. V.; Arion, V. B.; Burgess, J. *Template Synthesis of Macrocyclic Compounds*; Wiley-VCH: Weinheim, Germany, 1999.
(8) SCMs prepared from macrocyclic building blocks to date: (a) Bałanda, M.; Rams, M.; Nayak, S. K.; Tomkowicz, Z.; Haase, W.; Tomala, K.; Yakhmi, J. V. *Phys. Rev. B* **2006**, *74*, 224421. (b) Bernot, K.; Luzon, J.; Sessoli, R.; Vindigni, A.; Thion, J.; Richeter, S.; Leclercq, D.; Larionova, J.; van der Lee, A. *J. Am. Chem. Soc.* **2008**, *130*, 1619. (c) Zhang, D.; Zhang, L.-F.; Chen, Y.; Wang, H.; Ni, Z.-H.; Wernsdorfer, W.; Jiang, J. *Chem. Commun.* **2010**, *46*, 3550. (d) Venkatakrishnan, T. S.; Sahoo, S.; Bréfuel, N.; Duhayon, C.; Paulsen, C.; Barra, A.-L.; Ramasesha, S.; Sutter, J.-P. *J. Am. Chem. Soc.* **2010**, *132*, 6047. (e) Ishikawa, R.; Katoh, K.; Breedlove, B. K.; Yamashita, M. *Inorg. Chem.* **2012**, *51*, 9123. (f) Ding, M.; Wang, B.; Wang, Z.; Zhang, J.; Fuhr, O.; Fenske, D.; Gao, S. *Chem.—Eur. J.* **2012**, *18*, 915. (g) Richeter, S.; Larionova, J.; Long, J.; van der Lee, A.; Leclercq, D. *Eur. J. Inorg. Chem.* **2013**, *2013*, 3206.
(9) Feltham, H. L. C.; Clérac, R.; Powell, A. K.; Brooker, S. *Inorg. Chem.* **2011**, *50*, 4232.
(10) Verdaguer, M.; Bleuzen, A.; Marvaud, V.; Vaissermann, J.; Seuleiman, M.; Desplanches, C.; Scuiller, A.; Train, C.; Garde, R.; Gelly, G.; Lomenech, C.; Rosenman, I.; Veillet, P.; Cartier, C.; Villain, F. *Coord. Chem. Rev.* **1999**, *190−192*, 1023.
(11) Visinescu, D.; Madalan, A. M.; Andruh, M.; Duhayon, C.; Sutter, J. P.; Ungur, L.; den Heuvel, W. V.; Chibotaru, L. F. *Chem.—Eur. J.* **2009**, *15*, 11808.
(12) Przychodzeń, P.; Korzeniak, T.; Podgajny, R.; Sieklucka, B. *Coord. Chem. Rev.* **2006**, *250*, 2234.
(13) (a) Sieklucka, B.; Podgajny, R.; Korzeniak, T.; Nowicka, B.; Pinkowicz, D.; Kozieł, M. *Eur. J. Inorg. Chem.* **2011**, *2011*, 305. (b) Sieklucka, B.; Szklarzewicz, J.; Kemp, T. J.; Errington, W. *Inorg. Chem.* **2000**, *39*, 5156.
(14) (a) Sutter, J. P.; Dhers, S. C., J. P.; Duhayon, C. *C. R. Chim.* **2008**, *11*, 1200. (b) Sutter, J. P.; Dhers, S.; Rajamani, R.; Ramasesha, S.; Costes, J. P.; Duhayon, C.; Vendier, L. *Inorg. Chem.* **2009**, *48*, 5820. (c) Dhers, S.; Sahoo, S.; Costes, J.-P.; Duhayon, C.; Ramasesha, S.; Sutter, J.-P. *CrystEngComm* **2009**, *11*, 2078.
(15) Zhong, Z. J.; Seino, H.; Mizobe, Y.; Hidai, M.; Fujishima, A.; Ohkoshi, S.-i.; Hashimoto, K. *J. Am. Chem. Soc.* **2000**, *122*, 2952.
(16) (a) Visinescu, D.; Ie-Rang, J.; Madalan, A. M.; Alexandru, M.-G.; Jurca, B.; Mathonière, C.; Clérac, R.; Andruh, M. *Dalton Trans.* **2012**, *41*, 13578. (b) Gheorghe, R.; Madalan, A. M.; Costes, J.-P.; Wernsdorfer, W.; Andruh, M. *Dalton Trans.* **2010**, *39*, 4734.
(17) Visinescu, D.; Desplanches, C.; Imaz, I.; Bahers, V.; Pradhan, R.; Villamena, F. A.; Guionneau, P.; Sutter, J.-P. *J. Am. Chem. Soc.* **2006**, *128*, 10202.
(18) (a) Lim, J. H.; You, Y. S.; Yoo, H. S.; Yoon, J. H.; Kim, J. I.; Koh, E. K.; Hong, C. S. *Inorg. Chem.* **2007**, *46*, 10578. (b) Podgajny, R.; Korzeniak, T.; Stadnicka, K.; Dromzee, Y.; Alcock, N. W.; Errington, W.; Kruczala, K.; Balanda, M.; Kemp, T. J.; Verdaguer, M.; Sieklucka, B. *Dalton Trans.* **2003**, 3458. (c) Stefanczyk, O.; Korzeniak, T.; Nitek, W.; Rams, M.; Sieklucka, B. *Inorg. Chem.* **2011**, *50*, 8808. (d) Podgajny, R.; Pełka, R.; Desplanches, C.; Ducasse, L.; Nitek, W.; Korzeniak, T.; Stefanczyk, O.; Rams, M.; Sieklucka, B.; Verdaguer, M. *Inorg. Chem.* **2011**, *50*, 3213. (e) Song, X.-J.; Zhang, Z.-C.; Xu, Y.-L.; Wang, J.; Zhou, H.-B.; Song, Y. *Dalton Trans.* **2013**, *42*, 9505−9512.
(19) Dennis, C. R.; Van Wyk, A. J.; Basson, S. S.; Leipoldt, J. G. *Transition Met. Chem.* **1992**, *17*, 471.
(20) Sheldrick, G. M. *Acta Crystallogr., Sect. A* **2008**, *A64*, 112.
(21) Alvarez, S.; Alemany, P.; Casanova, D.; Cirera, J.; Llunell, M.; Avnir, D. *Coord. Chem. Rev.* **2005**, *249*, 1693.
(22) Ruiz-Martínez, A.; Casanova, D.; Alvarez, S. *Chem.—Eur. J.* **2008**, *14*, 1291.
(23) Addison, A. W.; Rao, T. N.; Reedijk, J.; van Rijn, J.; Vershoor, G. C. *J. Chem. Soc., Dalton Trans.* **1984**, 1349.
(24) Desiraju, G. R.; Steiner, T. *The weak hydrogen bond in structural chemistry and biology*; Oxford University Press: Oxford, U.K., 1999.
(25) Carlin, R. L.; Van Duyneveldt, A. J. *Acc. Chem. Res.* **1980**, *13*, 231.
(26) (a) Miyasaka, H.; Nakata, K.; Lecren, L.; Coulon, C.; Nakazawa, Y.; Fujisaki, T.; Sugiura, K.-i.; Yamashita, M.; Clérac, R. *J. Am. Chem. Soc.* **2006**, *128*, 3770. (b) Fatila, E. M.; Rouzières, M.; Jennings, M. C.; Lough, A. J.; Clérac, R.; Preuss, K. E. *J. Am. Chem. Soc.* **2013**, 9596.
(27) Labarta, A.; Iglesias, O.; Balcells, L.; Badia, F. *Phys. Rev. B* **1993**, *48*, 10240.
(28) Feltham, H. L. C.; Clérac, R.; Ungur, L.; Chibotaru, L. F.; Powell, A. K.; Brooker, S. *Inorg. Chem.* **2013**, *52*, 3236.
(29) (a) Coulon, C.; Clérac, R.; Wernsdorfer, W.; Colin, T.; Miyasaka, H. *Phys. Rev. Lett.* **2009**, *102*, 167204. (b) Bhowmick, I.; Hillard, E. A.; Dechambenoit, P.; Coulon, C.; Harris, T. D.; Clérac, R. *Chem. Commun.* **2012**, *48*, 9717.